Supplemental Material for "Transformations Based on Continuous Piecewise-Affine Velocity Fields"

Oren Freifeld, *Member, IEEE,* Søren Hauberg, *Member, IEEE,* Kayhan Batmanghelich, *Member, IEEE,* and Jonn W. Fisher III, *Member, IEEE,*

Abstract

In addition to the **attached two videos** (mentioned in the paper), this supplemental material contains:

1) Visualization of a CPA basis for a nominal type-II tessellation in 2D.
2) Proofs for the lemmas and theorems.

1 Visualization of a CPA Basis in the 2D Case

Figure 1 depicts the CPA fields that form a basis for $\mathcal{V}$ (a 2D case and a nominal type-I tessellation).

2 Proofs

In what follows, the operations of multiplication of a map by a scalar and addition of two maps are defined in the standard way; *i.e.*, if f and g are two $\Omega \to \mathbb{R}^n$ maps and $\alpha \in \mathbb{R}$, we define

$$(f+g) : \boldsymbol{x} \mapsto f(\boldsymbol{x}) + g(\boldsymbol{x}) \quad \text{and} \quad (\alpha f) : \boldsymbol{x} \mapsto \alpha f(\boldsymbol{x}) \,. \tag{1}$$

Proof of Lemma 1. **First**, we prove $\mathcal{V}'$ is linear by showing its closure under linear combinations. Let $\alpha \in \mathbb{R}$ and let f and f' be two PA maps, where $f : \boldsymbol{x} \mapsto A_{\gamma(\boldsymbol{x})}\widetilde{\boldsymbol{x}}$ and $f' : \boldsymbol{x} \mapsto A'_{\gamma(\boldsymbol{x})}\widetilde{\boldsymbol{x}}$. Now note that $\alpha f : \boldsymbol{x} \mapsto \alpha \left(A_{\gamma(\boldsymbol{x})}\widetilde{\boldsymbol{x}}\right) = \left(\alpha A_{\gamma(\boldsymbol{x})}\right)\widetilde{\boldsymbol{x}}$ and $f + f' : \boldsymbol{x} \mapsto A_{\gamma(\boldsymbol{x})}\widetilde{\boldsymbol{x}} + A'_{\gamma(\boldsymbol{x})}\widetilde{\boldsymbol{x}} = \left(A_{\gamma(\boldsymbol{x})} + A'_{\gamma(\boldsymbol{x})}\right)\widetilde{\boldsymbol{x}}$ are PA maps, as follows from the linearity of $\mathbb{R}^{n\times(n+1)}$. **Second**, since $\mathcal{V}$ is the intersection of two linear spaces, $\mathcal{V}$ and the space of $\Omega \to \mathbb{R}^n$ continuous maps, it follows that $\mathcal{V}$ is a linear space too. **Third**, that $D \triangleq \dim(\mathcal{V}) = (n^2+n) \times N_{\mathcal{P}}$ is trivial since any element of $\mathcal{V}'$ is defined by $N_{\mathcal{P}}$ (unconstrained) matrices of size $n \times (n+1)$. **Fourth**, assume $\mathcal{P}$ is a type-I tessellation. It follows that the values a CPA map takes at the vertices in a given cell uniquely define the A of that cell (and as we will see in the proof of Lemma 2, continuity of the field across inter-cell boundaries follows from the continuity at the vertices). Since in each one of these N_v vertices there are n degrees of freedom, it follows that $d \triangleq \dim(\mathcal{V}) = n \times N_v$. **Finally**, let $\mathcal{P}'$ be a tessellation that contains a cell which is not of type I. Then we can always partition this cell into type-I cells by simply adding vertices. In other words, for every non-type-I tessellation, $\mathcal{P}'$, there exists a type-I tessellation, $\mathcal{P}$ which is a refinement of $\mathcal{P}'$. Note that $\dim(\mathcal{V}_{\Omega,\mathcal{P}'}) < \dim(\mathcal{V}_{\Omega,\mathcal{P}})$. Let ${N_v}'$ stands for the number of vertices in $\mathcal{P}'$. Note that ${N_v}' < N_v$. It follows that $\dim(\mathcal{V}_{\Omega,\mathcal{P}}) < D$. □

Proof of Lemma 2. For concreteness, we prove it for $n = 2$ and type-I tessellations (*i.e.*, triangles). The other cases are handled exactly the same. Let $n = 2$ and let $\boldsymbol{v_A} \in \mathcal{V}'$, where $\boldsymbol{A} = (A_1, \ldots, N_{\mathcal{P}})$. While $\boldsymbol{v_A}$ is continuous on every cell, in general it is discontinuous on inter-cell boundaries. Consider two adjacent cells, U_i and U_j. Let us denote their 2 shared vertices by $\boldsymbol{x}_a$ and $\boldsymbol{x}_b$ and let A_i and A_j denote the corresponding 2×3 matrices. Continuity of $\boldsymbol{v_A}$ at $\boldsymbol{x}_a$ requires 2 (more generally, n) linear constraints on the values of A_i and A_j: one for the horizontal component of $\boldsymbol{v_A}$ and one for the vertical component of $\boldsymbol{v_A}$. Similarly, continuity at $\boldsymbol{x}_b$ requires another constraint pair. Thus, the continuity at both $\boldsymbol{x}_a$ and $\boldsymbol{x}_b$ implies the following 4 linear constraints:

- *O. Freifeld, K. Batmanghelich, and J.W. Fisher III are with the Computer Science and Artificial Intelligence Lab, Massachusetts Institute of Technology, Cambridge MA 02319, USA.*
  E-mail: {freifeld, kayhan, Fisher}@csail.mit.edu
- *S. Hauberg is with the Section for Cognitive Systems, DTU Compute, Kongens Lyngby, Denmark 2800.*
  E-mail: sohau@dtu.dk

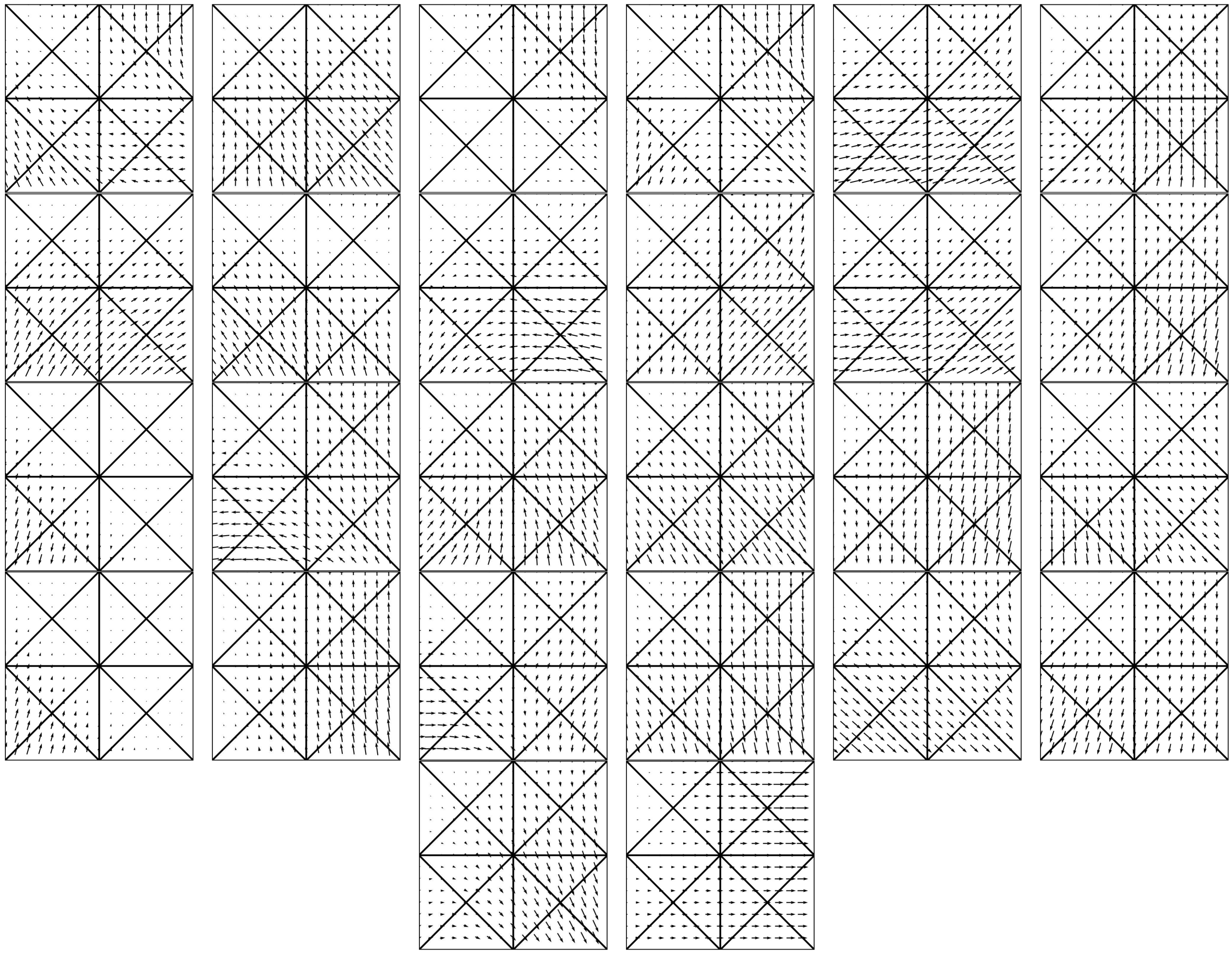

Fig. 1: The vector fields that constitute a 26-dimensional orthonormal basis of $\mathcal{V}$, obtained by SVD on B

$$\underbrace{\begin{bmatrix} \tilde{\boldsymbol{x}}_a^T & \mathbf{0}_{1\times 3} & -\tilde{\boldsymbol{x}}_a^T & \mathbf{0}_{1\times 3} \\ \mathbf{0}_{1\times 3} & \tilde{\boldsymbol{x}}_a^T & \mathbf{0}_{1\times 3} & -\tilde{\boldsymbol{x}}_a^T \\ \tilde{\boldsymbol{x}}_b^T & \mathbf{0}_{1\times 3} & -\tilde{\boldsymbol{x}}_b^T & \mathbf{0}_{1\times 3} \\ \mathbf{0}_{1\times 3} & \tilde{\boldsymbol{x}}_b^T & \mathbf{0}_{1\times 3} & -\tilde{\boldsymbol{x}}_b^T \end{bmatrix}}_{4\times 12} \underbrace{\begin{bmatrix} \mathrm{vec}(A_i) \\ \mathrm{vec}(A_j) \end{bmatrix}}_{12\times 1} = \mathbf{0}_{4\times 1} \text{ where } \mathrm{vec}(\left[\begin{smallmatrix} a_{11} & a_{12} & a_{13} \\ a_{21} & a_{22} & a_{23} \end{smallmatrix}\right]) \triangleq \begin{bmatrix} a_{11} \\ a_{12} \\ a_{13} \\ a_{21} \\ a_{22} \\ a_{23} \end{bmatrix} . \tag{2}$$

Continuity of $\boldsymbol{v}_{\boldsymbol{A}}$ at both $\boldsymbol{x}_a$ and $\boldsymbol{x}_b$ implies its continuity throughout their join, since for both affine maps, the values at a point on the join is the same convex combination of the values at $\boldsymbol{x}_a$ and $\boldsymbol{x}_b$; i.e., $A_i\widetilde{\boldsymbol{x}}_a = A_j\widetilde{\boldsymbol{x}}_a$ and $A_i\widetilde{\boldsymbol{x}}_b = A_j\widetilde{\boldsymbol{x}}_b$ imply

$$A_i(\lambda\widetilde{\boldsymbol{x}}_a + (1-\lambda)\widetilde{\boldsymbol{x}}_b) = A_j(\lambda\widetilde{\boldsymbol{x}}_a + (1-\lambda)\widetilde{\boldsymbol{x}}_b)\ \forall\lambda \in [0,1] . \tag{3}$$

Any $\boldsymbol{v}_{\boldsymbol{A}}$ whose A_i and A_j satisfy this linear system is thus continuous on $U_i \cup U_j$. Similar constraints may be enforced for other pairs of adjacent cells, and can be stacked together in an analogous equation:

$$\underset{4N_e\times 6N_{\mathcal{P}}}{L}\ \underset{6N_{\mathcal{P}}\times 1}{\mathbf{vec}(\boldsymbol{A})} = \mathbf{0}_{4N_e\times 1} \qquad\qquad \mathbf{vec}(\boldsymbol{A}) \triangleq \begin{bmatrix} \mathrm{vec}(A_1) \\ \vdots \\ \mathrm{vec}(A_{N_{\mathcal{P}}}) \end{bmatrix} \in \mathbb{R}^D = \mathbb{R}^{6N_{\mathcal{P}}} \tag{4}$$

where N_e is the number of shared line segments in $\mathcal{P}$ and L is the constraint matrix. Any $\boldsymbol{v}_{\boldsymbol{A}}$ whose $\boldsymbol{A}$ satisfies this linear system is thus everywhere continuous. We conclude that the null space of L, denoted by $\mathrm{null}(L)$, coincides with $\mathcal{V}$. $\square$

Recall that the columns of $\boldsymbol{B} = [\, \boldsymbol{B}_1 \ \dots \ \boldsymbol{B}_d \,] \in \mathbb{R}^{D\times d}$ denote the orthonormal basis of $\mathrm{null}(L)$ obtained via SVD.

Proof of Lemma 3. The matrix associated with $L_{\boldsymbol{v}^{\boldsymbol{\theta}}_{\mathrm{vert}} \mapsto \boldsymbol{\theta}}$ is a transition matrix between two known $d-$dimensional bases. $\square$

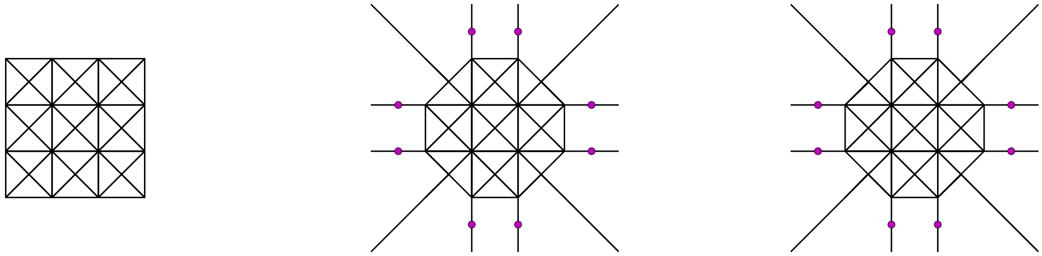

Fig. 2: Left: a triangular tessellation on compact region (a square in this case). Middle: Extending it to the whole of $\mathbb{R}^2$. The circles stand for auxiliary vertices where continuity is enforced (in addition to the continuity constraints at the original vertices, including the corners of the square). Right: Using the color scheme from the paper, and the extended tessellation, we show the horizontal component of some velocity field which is CPA on the whole of $\mathbb{R}^2$ (due to the additional constraints).

Example 1. For concreteness, let us look at a type-I tessellation when $n = 2$, the other cases being essentially identical. Let $\boldsymbol{x}_1$, $\boldsymbol{x}_2$ and $\boldsymbol{x}_3$ denote the vertices of a (non-degenerate) triangle, and let $\boldsymbol{v}_1$, $\boldsymbol{v}_2$ and $\boldsymbol{v}_3$ denote the values a CPA velocity field takes at these vertices, respectively. Letting $A = \left[\begin{smallmatrix} a_{11} & a_{12} & a_{13} \\ a_{21} & a_{22} & a_{23}\end{smallmatrix}\right]$ denote the matrix associated with this triangle, we have

$$\underbrace{\begin{bmatrix} \boldsymbol{v}_1 \\ \boldsymbol{v}_2 \\ \boldsymbol{v}_3 \end{bmatrix}}_{6\times 1} = \underbrace{\begin{bmatrix} A\widetilde{\boldsymbol{x}}_1 \\ A\widetilde{\boldsymbol{x}}_2 \\ A\widetilde{\boldsymbol{x}}_3 \end{bmatrix}}_{6\times 1} = \underbrace{\begin{bmatrix} \widetilde{\boldsymbol{x}}_1^T & \mathbf{0}_{1\times 3} \\ \mathbf{0}_{1\times 3} & \widetilde{\boldsymbol{x}}_1^T \\ \widetilde{\boldsymbol{x}}_2^T & \mathbf{0}_{1\times 3} \\ \mathbf{0}_{1\times 3} & \widetilde{\boldsymbol{x}}_3^T \\ \widetilde{\boldsymbol{x}}_3^T & \mathbf{0}_{1\times 3} \\ \mathbf{0}_{1\times 3} & \widetilde{\boldsymbol{x}}_3^T \end{bmatrix}}_{6\times 6} \begin{bmatrix} a_{11} \\ a_{12} \\ a_{13} \\ a_{21} \\ a_{22} \\ a_{23} \end{bmatrix} \Longrightarrow \begin{bmatrix} a_{11} \\ a_{12} \\ a_{13} \\ a_{21} \\ a_{22} \\ a_{23} \end{bmatrix} = \begin{bmatrix} \boldsymbol{v}_1 \\ \boldsymbol{v}_2 \\ \boldsymbol{v}_3 \end{bmatrix} \begin{bmatrix} \widetilde{\boldsymbol{x}}_1^T & \mathbf{0}_{1\times 3} \\ \mathbf{0}_{1\times 3} & \widetilde{\boldsymbol{x}}_1^T \\ \widetilde{\boldsymbol{x}}_2^T & \mathbf{0}_{1\times 3} \\ \mathbf{0}_{1\times 3} & \widetilde{\boldsymbol{x}}_3^T \\ \widetilde{\boldsymbol{x}}_3^T & \mathbf{0}_{1\times 3} \\ \mathbf{0}_{1\times 3} & \widetilde{\boldsymbol{x}}_3^T \end{bmatrix}^{-1} \tag{5}$$

(end of the example).

Proof of Lemma 4. We again focus on the case where $n = 2$, the other cases being similar. To enforce zero traces, we add to L rows derived from the following constraints:

$$\begin{bmatrix} 1 & 0 & 0 & 0 & 1 & 0 \end{bmatrix} \operatorname{vec}(A_c) = 0 \qquad\qquad \forall\, c \in \{1, \dots, N_{\mathcal{P}}\}\,. \tag{6}$$

Likewise, to nullify, *e.g.*, the horizontal component of the velocity across the rightmost boundary of $\Omega = [0, x_{\text{max}}] \times [0, y_{\text{max}}]$ we add rows derived from the constraints

$$\begin{bmatrix} \widetilde{\boldsymbol{x}}_a^T & \mathbf{0}_{1\times 3} \end{bmatrix} \operatorname{vec}(A_c) = 0 \tag{7}$$

for every vertex $\boldsymbol{x}_a$ of some cell U_c such that $\boldsymbol{x}$ is on the rightmost boundary of Ω. $\square$

Proof of Lemma 5. In case $n = 1$ and $\Omega = [x_{\text{xmin}}, x_{\text{xmax}}]$, we extend the leftmost and rightmost intervals to $-\infty$ and ∞, respectively, with adding no cells or constraints on $\boldsymbol{v}^{\boldsymbol{\theta}}$. If $n > 1$ and the tessellation is a regular one of type II (*i.e.*, the cells are hyperrectangles) the extension is trivial and be made by (non-compact) hyperrectnalges. Now consider type-I tessellations for $n \geq 2$. If $n = 2$ and Ω is a rectangle, we extend the outer cells of $\mathcal{P}$ (rendering them non-triangular) to cover the whole of $\mathbb{R}^2$ and add certain additional continuity constrains on $\boldsymbol{v}^{\theta}$. The process is best explained by Fig. 2. By an argument similar to the one used earlier to describe how continuity at two points ensures continuity of a PA field on their join, this process ensures the extended field is CPA over the whole of $\mathbb{R}^2$. Mathematically, the case with $n = 3$ can be handled in a similar-but-more-tedious way. However, unlike all the other 3D-related options mentioned in the paper, we did not implement this option for the 3D case. Rather, we opted to ensure the CPA property by imposing zero-boundary constraints. For $n > 3$, the general case is hard to implement, but, at least conceptually, can be done in a similar way to the above. However, we remind the reader that we stated in the paper that for $n > 3$ we use only type-II tessellations. $\square$

Before proceeding to the proofs of the theorems, recall that the solution, $t \mapsto \psi^t_{\boldsymbol{\theta},c}(\boldsymbol{x})$, to an ODE with an $\Omega \to \mathbb{R}^n$ *affine* velocity field, $\boldsymbol{x} \mapsto A_{c,\boldsymbol{\theta}}\widetilde{\boldsymbol{x}}$, is

$$\left[\begin{smallmatrix} \psi^t_{\boldsymbol{\theta},c}(\boldsymbol{x}) \\ 1 \end{smallmatrix}\right] \triangleq T_{A_{c,\boldsymbol{\theta}},t}\widetilde{\boldsymbol{x}}\,, \qquad A_{c,\boldsymbol{\theta}} \in \mathbb{R}^{n\times(n+1)}\,, \qquad T_{A_{c,\boldsymbol{\theta}},t} \triangleq \mathbf{expm}(t\widetilde{A_{c,\boldsymbol{\theta}}})\,, \qquad \widetilde{A_{c,\boldsymbol{\theta}}} = \begin{bmatrix} A_{c,\boldsymbol{\theta}} \\ \mathbf{0}_{1\times n+1} \end{bmatrix}. \tag{8}$$

Also recall that $\boldsymbol{\phi}^{\boldsymbol{\theta}}(\boldsymbol{x}, t)$ is given by the concatenation of such solutions

$$\boxed{\boldsymbol{\phi}^{\boldsymbol{\theta}}(\boldsymbol{x}, t) = (\psi^{t_m}_{\boldsymbol{\theta},c_m} \circ \ldots \circ \psi^{t_2}_{\boldsymbol{\theta},c_2} \circ \psi^{t_1}_{\boldsymbol{\theta},c_1})(\boldsymbol{x})}\,, \tag{9}$$

that $\exp(\boldsymbol{v}^{\theta}) \triangleq T^{\boldsymbol{\theta}}$ is defined via $T^{\boldsymbol{\theta}}(\boldsymbol{x}) = \boldsymbol{\phi}^{\boldsymbol{\theta}}(\boldsymbol{x}, 1)$, and that the compact notation in the boxed equation above hides an important detail: the number of the trajectory segments, their durations, and the cells involved (where a cell may appear more than once), *all depend on* $\boldsymbol{x}$. They all also depend on $\boldsymbol{\theta}$ and t, except the first cell; *i.e.*, $c_1 = \gamma(\boldsymbol{x})$; *i.e.*,

$$\boldsymbol{\phi}^{\boldsymbol{\theta}}(\boldsymbol{x}, t) = (\psi_{\boldsymbol{\theta}, c_{m_{\boldsymbol{x},\boldsymbol{\theta},t}}(\boldsymbol{x},\boldsymbol{\theta})}^{t_{m_{\boldsymbol{x},\boldsymbol{\theta},t}}(\boldsymbol{x},\boldsymbol{\theta},t)} \circ \ldots \circ \psi_{\boldsymbol{\theta}, c_2(\boldsymbol{x},\boldsymbol{\theta})}^{t_2(\boldsymbol{x},\boldsymbol{\theta},t)} \circ \psi_{\boldsymbol{\theta}, \gamma(\boldsymbol{x})}^{t_1(\boldsymbol{x},\boldsymbol{\theta},t)})(\boldsymbol{x}) \, . \tag{10}$$

Proof of Theorem 1. **Part (i).** For a given $\boldsymbol{x}$, the map $\boldsymbol{\theta} \mapsto \boldsymbol{v}^{\boldsymbol{\theta}}(\boldsymbol{x})$ is linear. Thus, $\boldsymbol{v}^{\boldsymbol{\theta}} = \boldsymbol{v}^{\alpha\boldsymbol{\theta}}/\alpha$. Moreover,

$$\xi^{\boldsymbol{\theta}}(\boldsymbol{x}, t) \triangleq \boldsymbol{\phi}^{\alpha\boldsymbol{\theta}}(\boldsymbol{x}, t/\alpha) = \boldsymbol{x} + \int_0^{t/\alpha} \boldsymbol{v}^{\alpha\boldsymbol{\theta}}(\boldsymbol{\phi}^{\alpha\boldsymbol{\theta}}(\boldsymbol{x}, \tau))\, d\tau = \boldsymbol{x} + \int_0^{t/\alpha} \alpha \boldsymbol{v}^{\boldsymbol{\theta}}(\boldsymbol{\phi}^{\alpha\boldsymbol{\theta}}(\boldsymbol{x}, \tau))\, d\tau \tag{11}$$

$$= \boldsymbol{x} + \int_0^{t} \boldsymbol{v}^{\boldsymbol{\theta}}(\boldsymbol{\phi}^{\alpha\boldsymbol{\theta}}(\boldsymbol{x}, \eta/\alpha))\, d\eta = \boldsymbol{x} + \int_0^{t} \boldsymbol{v}^{\boldsymbol{\theta}}(\xi^{\boldsymbol{\theta}}(\boldsymbol{x}, \eta))\, d\eta \tag{12}$$

and now observe that $\xi^{\boldsymbol{\theta}}(\cdot, t)$ coincides with $\boldsymbol{\phi}^{\boldsymbol{\theta}}(\cdot, t)$.

Part (ii). By applying the Picard-Lindelof theorem, and then extending the solution (to a finite t) we conclude that the trajectories do not intersect. From this it follows that $T^{\boldsymbol{\theta}}$ is invertible. Since $\boldsymbol{\theta} \mapsto \boldsymbol{v}^{\boldsymbol{\theta}}$ is linear, and since both $\mathbb{R}^d$ and $\mathcal{V}$ are linear spaces, we know that $\boldsymbol{v}^{-\boldsymbol{\theta}} \in \mathcal{V}$. Thus, by the definition of CPAB transformations, $T^{-\boldsymbol{\theta}} \in M$. We still, however, need to show that $T^{-\boldsymbol{\theta}} = (T^{\boldsymbol{\theta}})^{-1}$; *i.e.*, that $T^{-\boldsymbol{\theta}}$ is indeed the inverse of $T^{\boldsymbol{\theta}}$. By Eqn. (2) from the paper,

$$\boldsymbol{\phi}^{-\boldsymbol{\theta}}(\boldsymbol{\phi}^{\boldsymbol{\theta}}(\boldsymbol{x}, t), t) = \boldsymbol{\phi}^{\boldsymbol{\theta}}(\boldsymbol{x}, t) + \int_0^t \boldsymbol{v}^{-\boldsymbol{\theta}}(\boldsymbol{\phi}^{\boldsymbol{\theta}}(\boldsymbol{x}, \tau))\, d\tau = \boldsymbol{\phi}^{\boldsymbol{\theta}}(\boldsymbol{x}, t) - \int_0^t \boldsymbol{v}^{\boldsymbol{\theta}}(\boldsymbol{\phi}^{\boldsymbol{\theta}}(\boldsymbol{x}, \tau))\, d\tau = \boldsymbol{x} \tag{13}$$

where we used the fact the map $\boldsymbol{\theta} \mapsto \boldsymbol{v}^{\boldsymbol{\theta}}$ is linear (so $\boldsymbol{v}^{-\boldsymbol{\theta}} = -\boldsymbol{v}^{\boldsymbol{\theta}}$).

Part (iii). Since we showed that $(T^{\boldsymbol{\theta}})^{-1} = T^{-\boldsymbol{\theta}}$ and that $T^{-\boldsymbol{\theta}} \in M$, it is enough to show that any $T^{\boldsymbol{\theta}} \in M$ is differentiable. This is a known result for transformations obtained by integration of (stationary) Lipschitz-continuous velocity fields, but the CPA structure enables us to outline another proof, specialized to this case. Since $\boldsymbol{v}^{\boldsymbol{\theta}}$ is continuous, it follows that $\{t_i(\boldsymbol{x}, \boldsymbol{\theta}, t)\}_{i=1}^{m_{\boldsymbol{x},\boldsymbol{\theta},t}}$ are continuous functions of $\boldsymbol{x}$. The fact that $m_{\boldsymbol{x},\boldsymbol{\theta},t}$ changes with $\boldsymbol{x}$ does not change it. It just means a nominal t_i decreases continuously to zero or increases continuously from zero. Thus, taking the derivative of $\boldsymbol{\phi}^{\boldsymbol{\theta}}(\boldsymbol{x}, t)$ w.r.t. $\boldsymbol{x}$ results in summing terms of the form (notationally suppressing the dependency in t)

$$T_{\text{left},1} \, \frac{d\, \mathbf{expm}(\widetilde{t_i A_{c_i(\boldsymbol{x},\boldsymbol{\theta}),\boldsymbol{\theta}}})}{d\boldsymbol{x}} \, T_{\text{right},1} \, + T_{\text{left},2} \, \mathbf{expm}(\widetilde{t_i A_{c_i(\boldsymbol{x},\boldsymbol{\theta}),\boldsymbol{\theta}}}) \, T_{\text{right},2} \tag{14}$$

where $T_{\text{left},1}$, $T_{\text{left},2}$, $T_{\text{right},1}$ and $T_{\text{right},2}$ are $(n+1) \times (n+1)$ matrices that change continuously with $\boldsymbol{x}$ (and also depend on i and $\boldsymbol{\theta}$). Likewise, the matrix $\widetilde{t_i A_{c_i(\boldsymbol{x},\boldsymbol{\theta}),\boldsymbol{\theta}}}$ changes continuously with $\boldsymbol{x}$. Thus, $\frac{d\, \mathbf{expm}(\widetilde{t_i A_{c_i(\boldsymbol{x},\boldsymbol{\theta}),\boldsymbol{\theta}}})}{d\boldsymbol{x}}$ is continuous too.

Part (iv). A well-known result is that in the case of an affine velocity field, $\boldsymbol{x} \mapsto A\widetilde{\boldsymbol{x}}$, a zero-trace A implies that, for any (finite) t, the resulting transformation,

$$\boldsymbol{x} \mapsto \begin{bmatrix} I_{n\times n} & \mathbf{0}_{n\times 1} \end{bmatrix} \mathbf{expm}(t\widetilde{A})\widetilde{\boldsymbol{x}} \, , \tag{15}$$

is volume preserving. From a Lagrangian standpoint, one way to show this is by noting that the determinant of the Jacobian matrix is one (since it is equal to the determinant of $\mathbf{expm}(t\widetilde{A})$ which is one since the trace is zero – a known property of $\mathbf{expm}$). From an Eulerian standpoint, this can be shown by applying the Divergence Theorem since a zero trace of A implies that the velocity field has zero divergence, and thus, by the Divergence theorem, no mass leaves or enters the region of interest (subject to a regularity condition on the boundary of the region). In the CPA case, if all the A's have zero trace, then it can be similarly shown that the determinant of the Jacobian is still one (also verified numerically). However, it is easier to prove this using the Eulerian approach. Any region (whose boundary satisfies the regularity condition of the Divergence theorem) can be divided to smaller subregions such that each subregion is fully contained within some cell. In each such cell, the divergence of the field is zero and the Divergence theorem is applicable and thus the net inward flux (of mass, but by taking the density to be 1, it means volume) equals the net outward flux. Since the total flux is zero in every cell, the same holds for the entire region and we conclude the transformation is volume preserving. While this proof is restricted to regions whose boundary is regular, one can appeal to continuity arguments (approximating any non-regular boundary from inside and outside using regular boundaries) to prove the more general case.

Part (v). Any space whose elements are invertible $\Omega \to \Omega$ maps is nonlinear (w.r.t. the standard operations defined in Eqn. (1)), even if the maps themselves are linear[1]. To see that, note that the (constant) map, $\boldsymbol{x} \mapsto \mathbf{0}$, is the zero element of the linear space of all $\Omega \to \Omega$ maps (which contains M). This map is not invertible and is thus not in M. It follows that M is nonlinear since a linear subspace must contain the zero element of the larger linear space. As for the dimension, intuitively this follows from the fact that M is defined via the d-dimensional $\mathcal{V}$. We omit the formal proof (which is based on using $\exp$ to create a chart) as this is a standard result in differential geometry.

Part (vi). Since $\exp$ is smooth (particularity, it is uniformly continuous), it is enough to prove that $\mathcal{V}_{\Omega,\mathcal{P}_k}$ is dense in $C_\Omega^{\text{unif.}}$, the space of all uniformly-continuous velocity fields on Ω. Let $\boldsymbol{v} \in C_\Omega^{\text{unif.}}$. For every $k > 0$, there exists $\delta_k > 0$

1. *E.g.*, rotations in 3D are linear maps but $SO(3)$ is nonlinear.

such that $\|\boldsymbol{x}-\boldsymbol{y}\| < \delta_k \Rightarrow \|\boldsymbol{v}(\boldsymbol{x})-\boldsymbol{v}(\boldsymbol{y})\| < \frac{1}{k}$. Let $\mathcal{P}_1$ to be some tessellation (of Ω) such that each cell can be bounded within a ball of radius 1. For $k > 1$, define $\mathcal{P}_k$ to be some tessellation that is a refinement of $\mathcal{P}_{k-1}$ and that each of its cells cab be bounded within a ball of radius $\frac{1}{2k}$. Thus, for a fixed k, within each cell, $\|\boldsymbol{v}(\boldsymbol{x})-\boldsymbol{v}(\boldsymbol{y})\| < \frac{1}{2k}$. For $k \geq 1$, let $\boldsymbol{v}_k \in \mathcal{V}_{\Omega,\mathcal{P}_k}$ coincide with $\boldsymbol{v}$ on the vertices of $\mathcal{P}_k$. Thus, for a fixed k, within each cell, $\|\boldsymbol{v}_k(\boldsymbol{x})-\boldsymbol{v}_k(\boldsymbol{y})\| < \frac{1}{2k}$ (since $\boldsymbol{v}_k$ is affine within the cell). By the triangle inequality, within each cell, $\|\boldsymbol{v}_k(\boldsymbol{x})-\boldsymbol{v}(\boldsymbol{y})\| < \frac{1}{k}$. Letting k tend to ∞, we conclude that $\boldsymbol{v}_k$ converges to $\boldsymbol{v}$ uniformly. Thus, $\mathcal{V}_{\Omega,\mathcal{P}_k}$ is dense in $C_\Omega^{\text{unif.}}$. □

Proof of Theorem 2. In the notation below we drop the dependency in $\boldsymbol{\theta}$. Recall $n=1$. Thus, we can write $A_c = [a_c, b_c]$, and $\widetilde{A_c} = \left[\begin{smallmatrix} a_c & b_c \\ 0 & 0 \end{smallmatrix}\right]$. Also let $U_c = [x_c^{\min}, x_c^{\max}]$ denote the c^{th} interval. scalars a and b. For 2×2 matrices the matrix exponential is given in closed form [1]. If in addition, as we have here, the last row contains only zeros, this solution is given by

$$\mathbf{expm}\left(\begin{bmatrix} ta_c & tb_c \\ 0 & 0 \end{bmatrix}\right) = \begin{cases} \begin{bmatrix} e^{ta_c} & \frac{b_c(e^{ta_c}-1)}{a_c} \\ 0 & 1 \end{bmatrix} & \text{if } a_c \neq 0 \\ \\ \begin{bmatrix} 1 & tb_c \\ 0 & 1 \end{bmatrix} & \text{if } a_c = 0 \end{cases} \tag{16}$$

where we assumed $t \neq 0$ (if $t=0$ then we have $\mathbf{expm}(\mathbf{0}_{2\times 2}) = I_{2\times 2}$). Thus,

$$\psi_c^t(x) \triangleq \begin{bmatrix} 1 & 0 \end{bmatrix} \mathbf{expm}\left(\begin{bmatrix} ta_c & tb_c \\ 0 & 0 \end{bmatrix}\right)\begin{bmatrix} x \\ 1 \end{bmatrix} = \begin{cases} e^{ta_c}x + \frac{b_c(e^{ta_c}-1)}{a_c} & \text{if } a_c \neq 0 \\ \\ x + tb_c & \text{if } a_c = 0 \end{cases} \tag{17}$$

(note this includes the case of $t=0$). Without loss of generality, suppose $t > 0$. Let $\gamma(x) = c_1$ be the index of the interval containing x. Now suppose $\boldsymbol{v}(x) > 0$; i.e., the direction of the velocity at location x is rightward. Let $t_1(x)$ denote the time it takes to hit the right boundary of $U_{c_1} = [x_{c_1}^{\min}, x_{c_1}^{\max}]$:

$$t_1 \triangleq \min\left\{t : \psi_{c_1}^t(x) = x_{c_1}^{\max}\right\} \tag{18}$$

where, by convention, the minimum of an empty set is ∞. Solving for t_1,

$$t_1 = \infty \text{ if } \boldsymbol{v}(x_{c_1}^{\max}) \leq 0;\ \text{otherwise: } t_1 = \begin{cases} \frac{1}{a_{c_1}}\log\left(\frac{x_{c_1}+\frac{b_{c_1}}{a_{c_1}}}{x+\frac{b_{c_1}}{a_{c_1}}}\right) & \text{if } a_{c_1} \neq 0 \\ \\ \frac{x_{c_1}-x}{b_{c_1}} & \text{if } a_{c_1} = 0 \end{cases}. \tag{19}$$

If $t_1 > t$, then $\boldsymbol{\phi}^{\boldsymbol{\theta}}(x,t)$ is simply $\psi_{c_1}^t(x)$. Otherwise, it means we moved to next interval to the right, U_{c_1+1}, and we need to redo the process with $x_{c_1}^{\max}$ as the new starting point and $t-t_1$ instead of t. Since t is finite, this process will necessarily converge in a finite amount of steps, $m_{x,t}$. A loose upper bound on $m_{x,t}$ is $N_{\mathcal{P}} - c_1 + 1$. The case where $\boldsymbol{v}(x) < 0$ is handled similarly. Taken together,

$$\boldsymbol{\phi}(x;t) = (\psi_{c_m}^{t_m} \circ \ldots \circ \psi_{c_2}^{t_2} \circ \psi_{c_1}^{t_1})(x) \tag{20}$$

where for $2 \leq i \leq m$, $c_i = c_{i-1} + \operatorname{sign}(\boldsymbol{v}(x))$, while m and $\{t_i\}_{i=1}^m$ are found by the aforementioned procedure. □

REFERENCES

[1] D. S. Bernstein and W. So, "Some explicit formulas for the matrix exponential," *Automatic Control, IEEE Transactions on*, vol. 38, no. 8, pp. 1228–1232, 1993.